Analysis of Fatigue Crack Evolution using In-Situ Testing

Hassan Alqahtani[1,2], Eric Keller[1], Asok Ray[1,3,4], Amrita Basak[1,4]

[1] Department of Mechanical Engineering, Pennsylvania State University, University Park, PA 16802

[2] Department of Mechanical Engineering, Taibah University, Medina, KSA, 42353

[3] Department of Mathematics, Pennsylvania State University, University Park, PA 16802

[4] Corresponding authors, email: axr2@psu.edu & aub1526@psu.edu

Abstract

The objective of the current work is to investigate the feasibility of an in-situ technique to characterize the evolution of fatigue failure in conventionally manufactured aluminum parts in real time. An in-situ fatigue testing setup integrated with ultrasonic transducers and a digital microscope allows for the systematic study of fatigue crack evolution in aluminum specimens. The resulting data from experimentation, characterization, and analysis are integrated to gain unprecedented insights into the evolution of fatigue failure in wrought aluminum parts. The learning from this work will be further implemented on additively manufactured specimens.

Keywords

Fatigue damage, crack initiation, ultrasonic test, digital microscope, signal attenuation, discrete wavelet transform.

Introduction

Fatigue damage is one of the ubiquitous sources of structural degradation during both nominal and off-nominal operations in engineering components. While model-based computational methods for assessing structural damage evolution are available, difficulty in achieving the required accuracy due to inadequacy in capturing the dynamical behavior of fatigue damage at the grain level makes them difficult to solely rely on. The random distribution of microstructural flaws such as inclusions and defects produce a wide uncertainty in the crack initiation phase [1]. Such defects become even more critical in additively manufactured (AM) components which typically consist of an array of microstructural irregularities such as voids and pores that are radically different from their cast counterparts [2]. The defects coupled with microstructural anisotropy in AM-fabricated parts render the prediction of fatigue crack evolution near to intractable through computational modeling only.

Most of the existing research on fatigue analysis relies on performing the experimentation till the specimen is cracked and thereafter carrying out the post-inspection of the cracked surface. Such methods fail to accurately capture the crack initiation phenomena [3]. A recent publication suggested that the lowest performing components failed at easily observable pores, but the higher

performing components were more ambiguous with their failure mechanisms. This is due to the complex interplay between microstructural irregularities and anisotropy [4]. Studying the crack evolution in the material structure, therefore, is critical for avoiding the structural damage. Crack nucleates at the grain boundaries, and then it flows along the direction of the slip band. The maximum crack initiation length is usually less than 0.25 mm [1]. In this paper, the presence of the crack initiation is determined by finding the smallest measurable crack size on the notch surface of the specimen [5, 6].

Crack initiation is highly influenced by the defects which are created during the manufacturing process. In this study, aluminum alloy specimens fabricated via wrought processing are chosen to be investigated. Fatigue loads are generated by an MTS test machine (831.10 Elastomer Test system), and the fatigue initiation of the metallic structure is monitored by ultrasonic test (UT) measurements and a digital microscope. UT is considered to be one of the best methods of nondestructive testing (NDT) that can detect the crack initiation and monitor the crack propagation. The ultrasound defines as the sound waves which have a frequency above the audible range (<20 kHz). In UT, the ultrasonic waves diffuse inside the specimens and detect microstructure defects such as voids and small cracks. It is well known that UT is efficient to identify the onset of the crack growth since its wavelength is very short and it can be reflected due to internal defects of the materials. To increase the credibility of UT results, the digital microscope is used in conjunction with UT to monitor the crack on the specimen surface [7].

The onset of the ultrasonic signal attenuation is considered to be evidence of the crack initiation. To identify the onset of signal attenuation, the discrete wavelet transform (DWT) is applied to analyze the signals of the UT [8]. DWT can decompose the signal into the approximation coefficients and detail coefficients. The approximation coefficients represent the low-frequency signals while the detail coefficients represent the high-frequency signals.

The contributions of this study are summarized as follows:

1. Validation of the ultrasonic testing (UT) measurements using digital microscopic data
2. Implementation and demonstration of the discrete wavelet transform concept on UT signals data.

This paper is organized in five sections. Section 2 illustrates the concept and the mathematical background of the discrete wavelet transform. Section 3 describes the experimental procedure. Section 4 discusses the results from UT, DWT, and the digital microscope. Section 5 summarizes the results and presents the future work. If successful, the framework developed in this study can be implemented to qualify components produced by AM.

Mathematical Background - discrete wavelet transform

In the wavelet transform, the signal $f(t)$ is multiplied by a scaled parameter and shifted by a wavelet function $k(t)$. The wavelet transform coefficients $K(a,b)$ can be defined as:

$$K(a, b) = \int_{-\inf}^{\inf} f(t)\left(\frac{1}{\sqrt{a}}\right) \psi\left(\frac{t-b}{a}\right) dt \qquad (1)$$

Here, a is the scaling parameter and b is a shifting parameter. The factors that make the wavelet transform valuable are the scaling parameter and the wavelet function $\psi\left(\frac{t-b}{a}\right)$. The scaling parameter has a significant role to obtain the high-frequency components and low-frequency components of the signal $f(t)$ while the shifted parameter is used to shift the wavelet widow overall time to cover the whole signal $f(t)$. The small scaling parameter can be used to determine the high-frequency components, and it is related to a compressed wavelet function. On the contrary, the large scaling parameter can be used to determine the low-frequency components, and it is related to an expanded wavelet function. Therefore, the large scaling parameter is used for a general analysis while the small parameter is used for a specific analysis [8, 9].

The discrete wavelet transform can be used when the signal is a digital signal $f(l)$, where l = 0,1,2,...,l . As shown in Figure 1, the DWT process is divided into two sections, and it shows two-channel filter banks. The first section is called analysis filter bank and the second section is called synthesis filter bank. In this study, the analysis filter section has been studied. In the analysis filter bank of Figure 1, the original s(n) is decomposed into two channels (high pass filter and low pass filter). Since the frequency range of the decomposed digital signal is half the frequency range of the original digital (s(n)), the output of each filter is down sampled by two.

$$y_0(k) = \sum_n s(n)h(0,2k - n) \qquad (2)$$

$$y_1(k) = \sum_n s(n)h(1,2k - n) \qquad (3)$$

The level of this step is the 1st level. We assumed that if i=0, the filter is a low pass filter, and it produces the approximation coefficients of DWT where the low-frequency components of the signal $s(n)$ are related to the approximation coefficients. However, if i=1, the filter is considered to be a high pass filter, and it represents the detail coefficients of DWT.
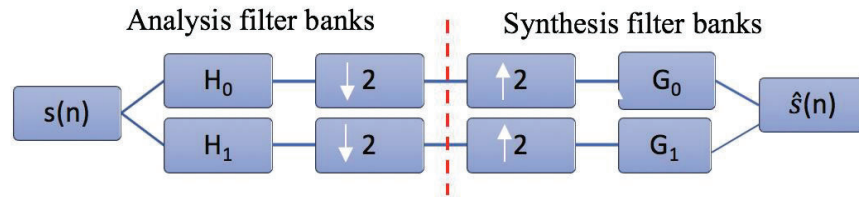

Figure 1. Block diagram of the analysis and synthesis filter banks of two-channel.

For multilevel filter bank analysis, eq. (2) and eq. (3) can be modified as:

$$y_0^{(P)}(k) = \sum_n s(n)h^{(P)}(0,2^P k - n) \qquad (4)$$

$$y_1^{(p)}(k) = \sum_n s(n)h^{(p)}(1,2^p k - n) \qquad p = 1,2,3, \ldots, P \qquad (5)$$

In this study, the desired outputs are obtained at level four of the filter bank analysis. Figure 2 illustrates the block diagram of the analysis filter bank that is implemented in this study.
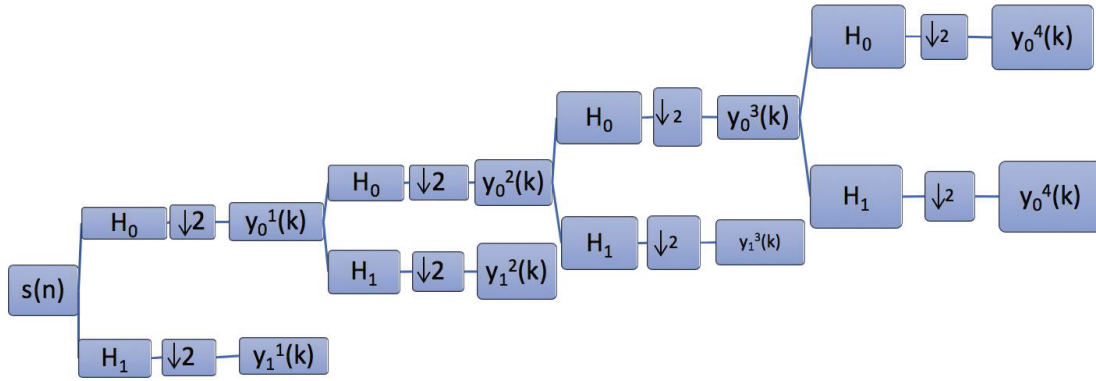
Figure 2. Block diagram of the level-4 analysis filter banks.

From Figure 2, H_0 represents the lowpass filter and H_1 represents the highpass filter. The desired outputs $y_0^4(k)$ (level 4 approximation coefficients of DWT) and $y_1^4(k)$ (level 4 details coefficients of DWT) are obtained from eq. 6 and eq. 7

$$y_0^{(4)}(k) = \sum_n s(n)h^{(4)}(0,16k-n) \tag{6}$$

$$y_1^{(4)}(k) = \sum_n s(n)h^{(4)}(1,16k-n) \tag{7}$$

Here, the number (4) between the parentheses is related to the level number. [1]

<u>Description of experimental apparatus</u>

Wrought specimens of 7075-T6 aluminum alloy are used in this study. The specimens are 3 mm thick and 50 mm wide. A notch is incorporated at the edge with dimensions of (1 mm × 3.5 mm) as shown in Figure 3. The experimental apparatus, as shown in Figure 4, is used to detect the crack evolution. Specimens are subjected to tension-tension load cycles at 60 Hz, and the load is generated by the MTS test machine. The target set point of the load is 8,000 N and the amplitude load is 4,000 N where the load fluctuates between 10,000 N and 6,000 N. In UT, ultrasonic wave is injected to the metallic specimen by a piezoelectric transducer called transmitter, and the transmitted signals are detected by another piezoelectric transducer called receiver which is located on the other side of the notch. When the crack propagates, the signals start to attenuate since part of the signals are reflected and not transmitted to the receiver as shown in Figure 6. Furthermore, a digital microscope is used in conjunction with UT to monitor the crack evolution behavior and to provide an evidence for the attenuation of the signals. The digital microscope magnification that is used in this study is 50x.
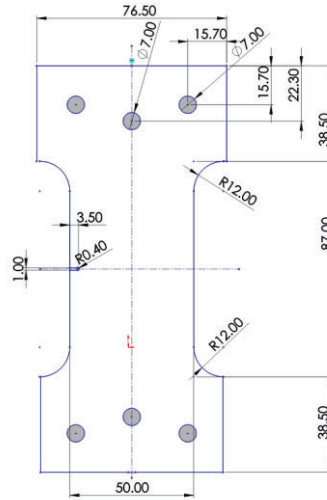
**Figure 3. Specimen geometry used for fatigue testing.**
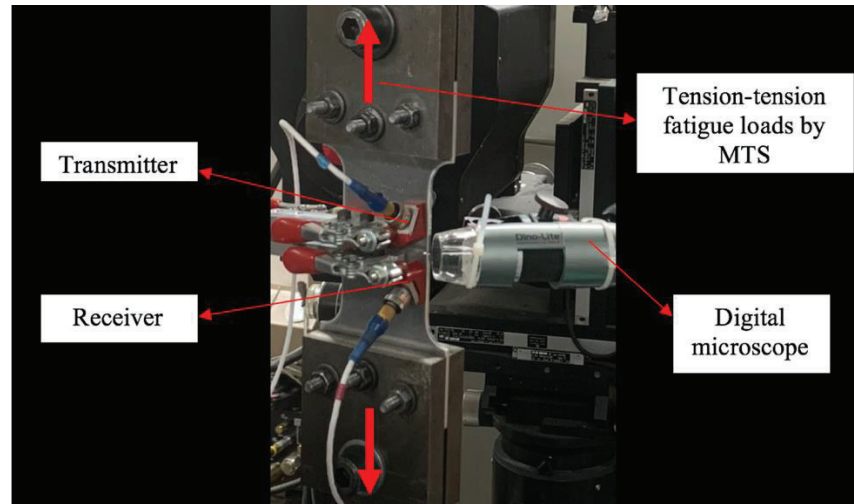

Figure 4. Experimental apparatus for crack detection.

Experimental results and discussion

The digital microscope starts to observe the crack on the notch surface at almost 44,939 loading cycles while the UT does not show the attenuation in the signal at the same moment as shown in Figure 5 and Figure 6. As shown in Figure 6, the global ultrasonic data shows the signal attenuation at around 48,680 loading cycles. Thus, the delay of crack propagation detection using global ultrasonic data is 3,741 loading cycles. The first reason for the crack delay detection in the global ultrasonic data is that the signal attenuates only when the crack is open. At the crack initiation, the crack opens at maximum load, 10,000 N, and it closes at the minimum load, 6,000 N. The tremendous amount of the data generated during UT is another reason for the delay in detection. The total number of the signals that are measured is almost 19,404 signals with each signal having 51 measured points.

To overcome the delay detection of the crack in the global ultrasonic data, the local analysis of the ultrasonic data needs to be computed instead of the global analysis. Thus, the DWT is applied to analysis the local UT data.


(a) (b)
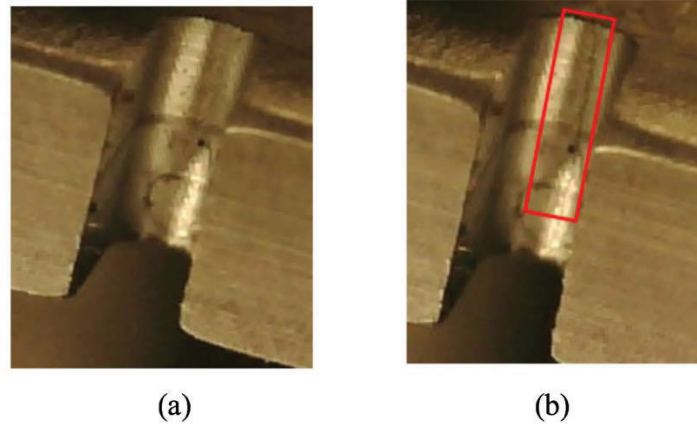
Figure 5. Digital microscope image of the notch surface at (a) 0 loading cycle and (b) 44939 loading cycles.
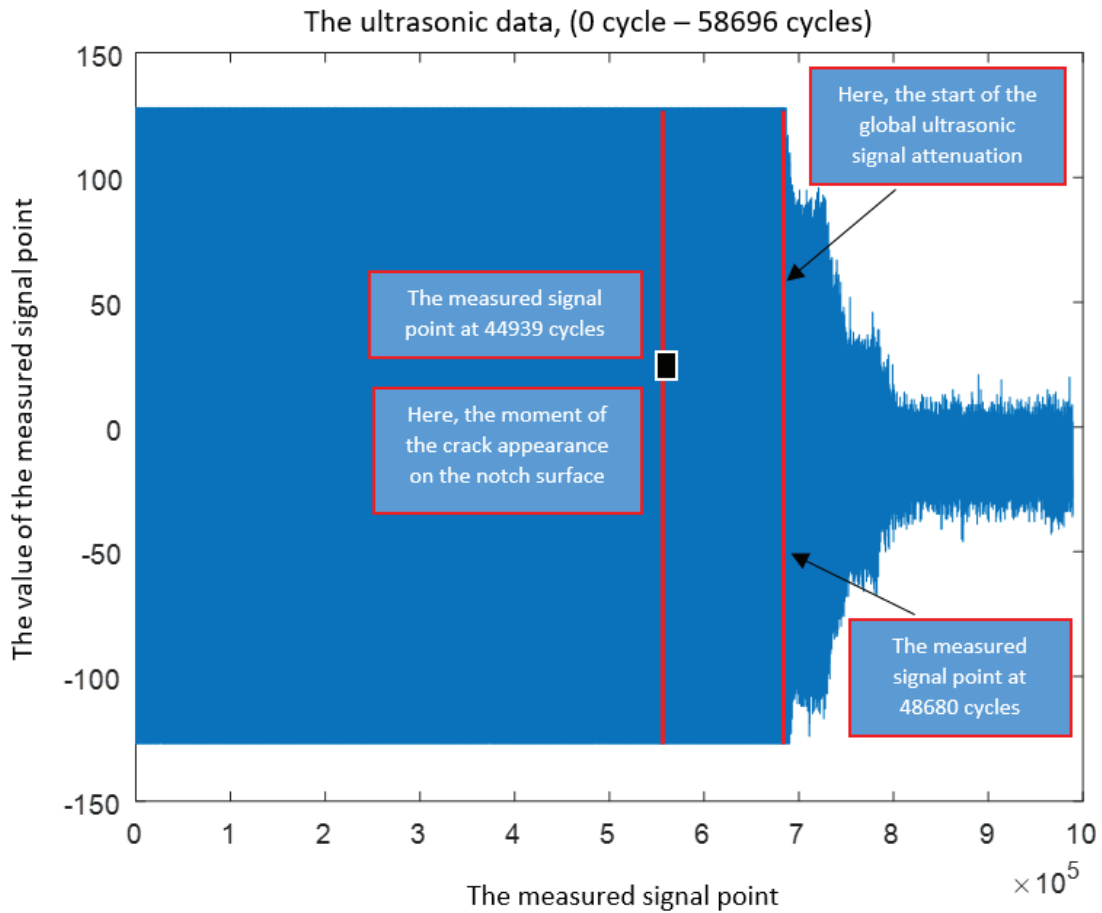

Figure 6. Measured points of the ultrasonic signals, from 0 loading cycle to 58,696 loading cycles.

The block diagram process of Figure 2 is illustrated in this section as follows:

1. The original signal *s(n)* is obtained from UT, and the length of this signal is almost 566,400 points which represent the measured signal points from the beginning of the experiment until the appearance of the crack on the notch surface as shown in Figure. 7(a).

2. The input of the 1st level is the original signal. In the 1st of the analysis filter banks, *s(n)* is decomposed into approximation output ($y_0^1(k)$) and detail output ($y_1^1(k)$) as shown in Figure 7(b).

3. The 1st level approximation output ($y_0^1(k)$) becomes the input signal values of the 2nd level of the analysis filter banks. $y_0^1(k)$ is decomposed into approximation output ($y_0^2(k)$) and detail output ($y_1^2(k)$) as shown in Figures 8(a) and 8(b).

4. Step 3 can be applied to the 3rd level and the 4th level of the analysis filter banks where the input signal of each level is the approximation output of the previous level, and in each level, the input signal is decomposed into new approximation output and new detail output as shown in Figures 9(a), 9(b), 10(a), and 10(b).
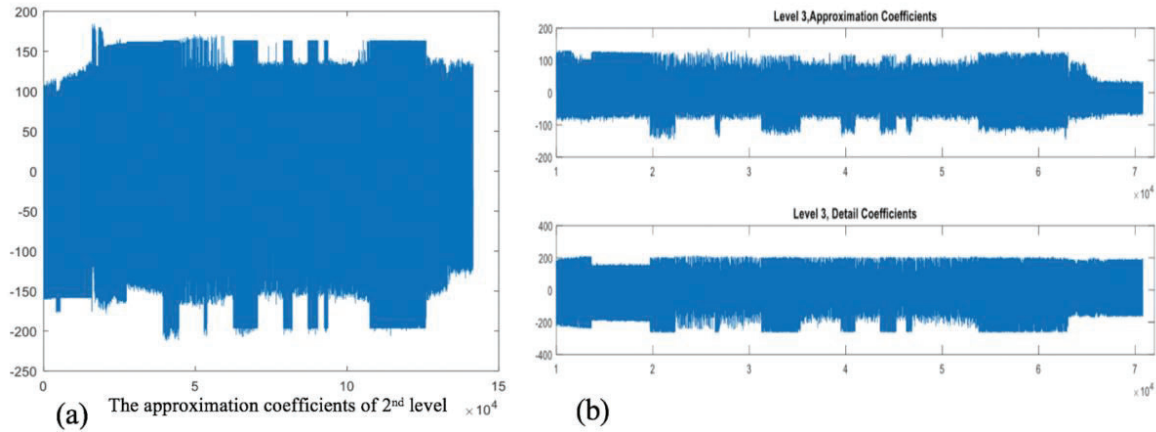

(a)   (b)
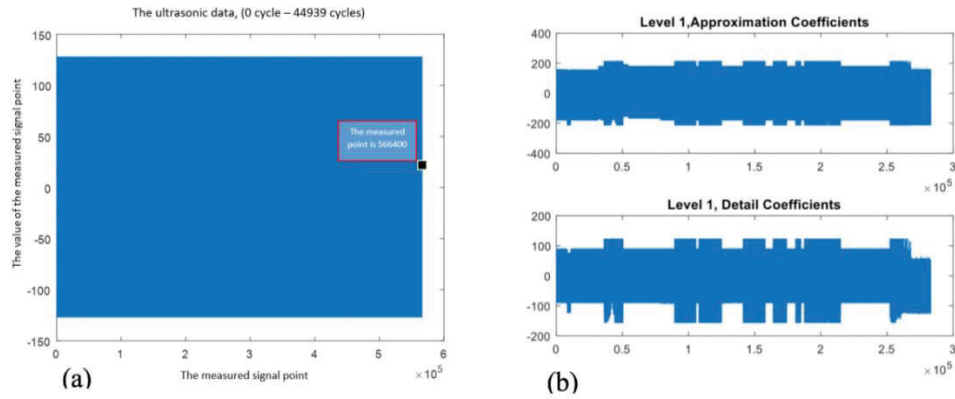
Figure 7. (a) Measured points of the ultrasonic signals, from 0 cycles to 44,939 loading cycles and (b)1st level of the approximation coefficients and detail coefficients of DWT.
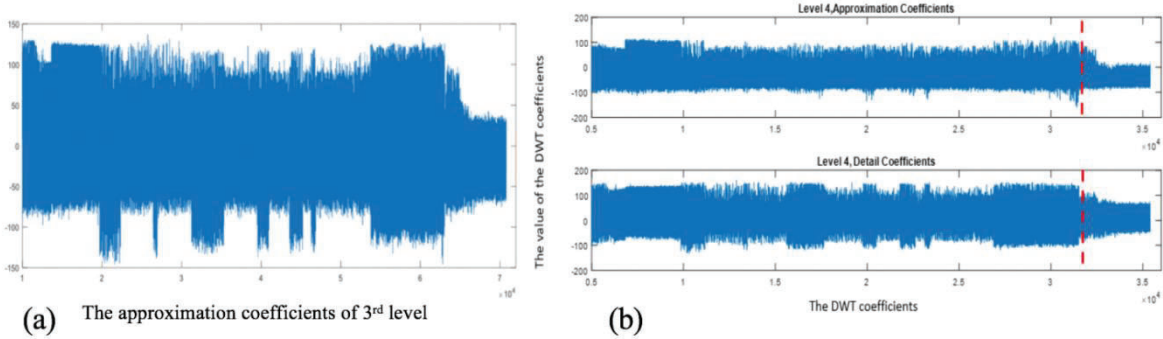

(a)   (b)
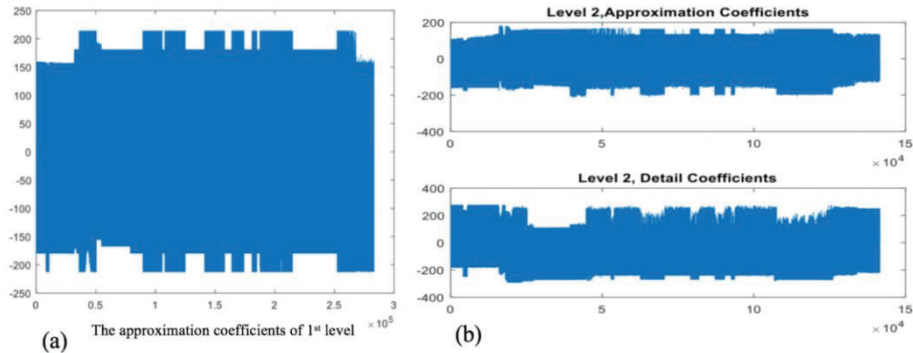
Figure 8. (a) 1st level approximation output, the input signal of the 2nd level and (b) 2nd level of the approximation coefficients and detail coefficients of DWT.

Figure 9. (a) 2ⁿᵈ level approximation output, the input signal of the 3ʳᵈ level and (b) the 3ʳᵈ level of the approximation coefficients and detail coefficients of DWT.

Figure 10. (a) 3ʳᵈ level approximation output, the input signal of the 4ᵗʰ level and (b) 4ᵗʰ level of the approximation coefficients and detail coefficients of DWT.

As shown in Figure 9(b), The third-level wavelet decomposition of ultrasonic signals provides a clear reduction in the approximation coefficients output which is a sign of the crack initiation since the crack appears on the surface notch at 44,939 loading cycles and the approximation output of the 3ʳᵈ level decreases before 44,939 loading cycles. To increase the validity of the 3ʳᵈ level results, we decompose the approximation output of the 3ʳᵈ level into new approximation coefficients output and new detail coefficients output. The outputs of the 4ᵗʰ level of the analysis filter bank emphasize the observations at the 3ʳᵈ level where the approximation coefficients reduce before 44,939 loading cycles as shown in Figure 10(b).

Conclusions and future work

In this study, the importance of detecting crack initiation has been described. The use of the ultrasonic to detect the crack initiation in aluminum specimens proved the value of UT. DWT clearly identify the crack initiation by applying the multilevel signal decomposition. The third-level wavelet decomposition is suitable to determine the crack initiation where the approximation coefficients clearly identify the sudden drop of the signal. The metallic structure can be maintained when the crack is observed during the crack initiation stage, but the digital microscope detects only the crack propagation. Therefore, more advanced measurement instrument such as Alicona confocal microscope which can monitor the crack initiation needs to

be used. Alicona is a 3D measurement system, and it is capable to measure the surface roughness from 3D magnified image.

References

[1] Gupta S. Behavioral pattern identification for structural health monitoring in complex systems. 2006.

[2] Basak A, Das S. Epitaxy and Microstructure Evolution in Metal Additive Manufacturing. Annual Review of Materials Research 2016;46:125-49.

[3] DebRoy T, Wei H, Zuback J, Mukherjee T, Elmer J, Milewski J, et al. Additive manufacturing of metallic components–process, structure and properties. Progress in Materials Science 2018;92:112-224.

[4] Sheridan L, Scott-Emuakpor OE, George T, Gockel JE. Relating porosity to fatigue failure in additively manufactured alloy 718. Materials Science and Engineering: A 2018;727:170-6.

[5] Schneider R, Heine B, Grant RJ. Mechanical Behaviour of Commercial Aluminium Wrought Alloys at Low Temperatures. In: Monteiro WA, editor. Light Metal Alloys Applications: IntechOpen; 2014.

[6] Suresh S. Fatigue of materials: Cambridge university press; 1998.

[7] Schmerr LW. Fundamentals of ultrasonic nondestructive evaluation: Springer; 2016.

[8] Lee B. Application of the discrete wavelet transform to the monitoring of tool failure in end milling using the spindle motor current. The International Journal of Advanced Manufacturing Technology 1999;15:238-43.

[9] Weeks M, Bayoumi M. Discrete wavelet transform: architectures, design and performance issues. Journal of VLSI signal processing systems for signal, image and video technology 2003;35:155-78.